An Argument for the Use of Multiple Segment Stents in Curved Arteries

Saeid Kasiri[1]
e-mail: kasirigs@tcd.ie

Daniel J. Kelly

Trinity Centre for Bioengineering,
University of Dublin,
Parsons Building,
College Green,
Dublin 2, Ireland

Stenting of curved arteries is generally perceived to be more challenging than straight vessels. Conceptually implanting multiple shorter stents rather than a single longer stent into such a curved artery represents a promising concept, but little is known about the impact of such an approach. The objective of this study is to evaluate the effectiveness of using a multiple segment stent rather than a single long stent to dilate a curved artery using the finite element method. A double segment stent (DSS) and a single segment stent (SSS) were modeled. The stents were compared when expanded into a model of a curved artery. The model predicts that the DSS provides higher flexibility, more conformity, and lower recoil in comparison to the SSS. The volume of arterial tissue experiencing high levels of stress due to stent implantation is also reduced for the DSS. It is suggested that a multiple segment stenting system is a potential solution to the problem of higher rates of in-stent restenosis in curved arteries and mechanically challenging environments. [DOI: 10.1115/1.4004863]

Keywords: curved artery, multiple stent, finite element method, restenosis

Introduction

In-stent restenosis (ISR) still remains a greater problem in diseased arteries of more complex geometry such as the right coronary and certain peripheral arteries. For example, stenting in a diseased iliac artery with high curvature of about 0.085 mm^{-1} [1] is typically more complicated [2] compared to a healthy iliac artery with a small curvature of 0.01 mm^{-1} [3]. There is a higher risk of vessel injury when stenting a curved artery, with neointimal thickening and ISR strongly correlated to the level of vessel injury [4]. Endothelium damage initiates an inflammatory response resulting in neointima hyperplasia [5]. Damage to the endothelium during angioplasty and stenting is at least partially a result of the high stress and/or strain imposed on the artery wall during the implantation procedure or during the lifetime of the device. This implies that the design of stents is one of the important factors that can affect the restenosis rate [6]. Flexibility after expansion, radial strength, elastic recoil, conformity, and metal to tissue ratio are some of the known factors of stent design that affect restenosis.

Stenting a curved artery is generally considered to be a more complicated procedure compared to straight arteries [2,7]. Adverse mechanical effects such as strut prolapse, flattening, and kinking may occur during stent placement in such an artery [8]. In addition, an abrupt change in the curvature of bent arteries due to the rigidity of the stent extremes leads to stress concentrations within the arterial wall [9]. The relatively high rigidity of the expanded stent compared to the artery can also result in injury to the artery and nonconformity to the vessel wall resulting in ISR [9].

Implanting a stent in the curved artery may also cause vessel straightening [8,10]. Vessel straightening reduces as stent flexibility increases. In an attempt to address this problem, different stent link elements have been introduced in new stent designs in order to increase stent flexibility. The link elements are bridges that connect two cells or struts of a stent and are usually in shapes of "S", "V", "W" etc. They have been designed to remain in the elastic zone of the material during implantation and also under in vivo conditions. If a stent is bent, the link elements at the outer curvature of the stented vessel are pulled apart. Under these circumstances, the links along the inner curvature become closer due to compression. This can sometimes result in poor conformity of the stent to the vessel wall [9].

In order to provide improved stent flexibility and conformity and lower vessel straightening, an alternative approach to stenting such arteries is required. It is proposed that implanting a multiple segment stent (MSS) would overcome many of the problems currently associated with stenting curved arteries. The objective of this study is to use the finite element method to investigate the effectiveness of such an approach. Finite element (FE) analysis has been extensively employed to study stent-artery interactions [11–13] and to optimize stent designs [14,15]. An optimized stent design should at least [1] minimize tissue injury, [2] maximize conformity to decrease the blood flow turbulence, [3] provide sufficient radial strength to prevent recoil while, and [4] having the minimum metal to artery ratio to reduce the risk of thrombosis. In this proof-of-principal study, the effectiveness of using MSS instead of one longer single segment stent (SSS) will be evaluated in terms of these criteria using the finite element method. If it can be demonstrated that an MSS is superior in this context, it will provide support for further *in silico* and in vivo investigations of this stenting concept in curved arteries.

Method

Geometry. The artery was modeled as an ideal curved tube with the inner curvature of 0.1 mm^{-1}. The inner diameter of the arterial tube was assumed to be 6 mm with an overall length of 22.7 mm. Three different layers, intima, media, and adventitia were considered. The balloon was modeled as an ideal cylinder (Fig. 1).

Two stents were modeled, an SSS and a DSS. In order to compare the effects of a DSS, the parameters of two stents such as strut width and thickness are kept the same for both stents. Also, the expanded length and diameter are similar for both types of the stents. The stents have a nominal diameter of 8 mm and strut thickness of 120 μm. The strut width is designed to be about 100 μm. In order to prevent overlapping between the segments, an interlock mechanism was employed in the design of the DSS (Fig. 1).

Material Model. The artery thickness was assumed to be 1 mm with a thickness ratio for the Int:Med:Adv of 13:32:55 [16]. Each layer was modeled as an incompressible isotropic hyperelastic material using a 3rd order Mooney-Rivlin equation [15]. The material models for the arteries were based on data obtained for human iliac arteries (Table 1) [16]. The layers were meshed using linear hexahedron elements (C3D8R) in Abaqus6.8®.

A simplified balloon model was used to simulate the expansion of the stent. An idealized shell cylinder with a two parameters Mooney-Rivlin with $C10 = 1031.7$ (kPa) and $C01 = 3692.66$ (kPa) was used to model the balloon. Linear quadrilateral elements (S4R) were employed to mesh the balloon.

The stent was modeled as stainless steel, 316L. The thickness of the stent struts was assumed to be 120 μm. It means that there

[1]Corresponding author.

Contributed by the Bioengineering Division of ASME for publication in the Journal of Biomechanical Engineering. Manuscript received February 1, 2011; final manuscript received August 2, 2011; published online September 15, 2011. Editor: Michael Sacks.

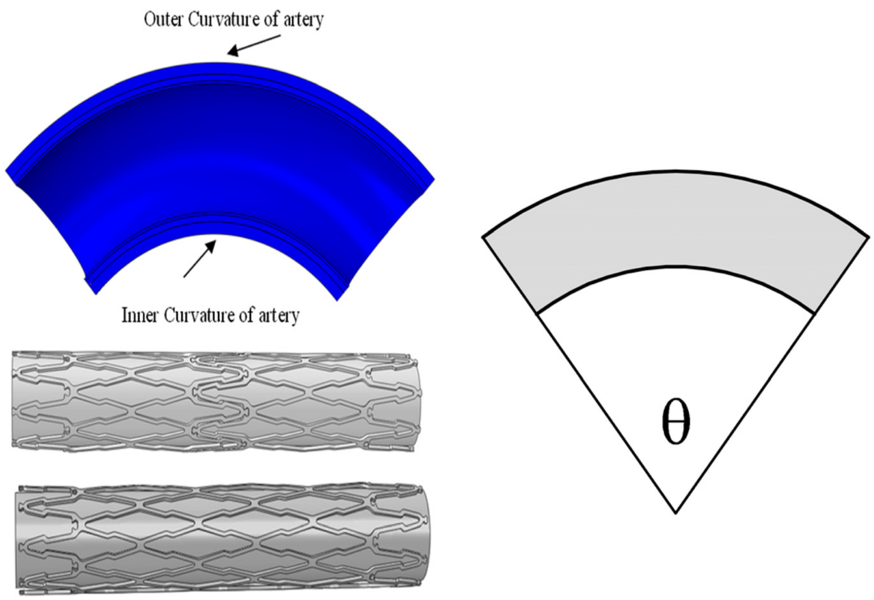

Fig. 1 Geometry model of (top left) unreformed curved artery, (middle left) DSS on the balloon and (bottom left) SSS on balloon. (right) Angle of artery curve, Changes in the angle shows the level of straightening due to stenting.

are only a few grains allocated along the width of the strut. The material properties; therefore, were obtained from micro-specimen tests. Values for Young's modulus, yield and ultimate stress are 193 GPa, 207 MPa, 520 MPa, respectively, and Poisson ratio and ultimate strain of 0.27 and 0.45 were employed [17]. The Von-Mises criterion was used to model the plasticity of stainless steel.

Boundary Conditions. Abaqus6.8 ® (Dassault Systèmes Simulia Corp., Providence, RI) with general dynamic analysis was employed for simulation. Half of the model was simulated due to the symmetry. Symmetric boundary conditions were applied where appropriate. The two ends of the balloon were constrained in its circumferential and axial directions. The balloon inflation was modeled by applying displacement on the inner surface of the balloon. Displacement was then reduced to zero to model the balloon deflation. Contact was modeled between two segments of the DSS during the balloon inflation and also between the stents with artery and balloon. A penalty method with the friction factor of 0.12 between the surfaces was used to model the contact. To evaluate the quasi static response, in the general dynamic explicit model, the energy balance was monitored to ensure that the kinetic energy of the deforming material was smaller than 5% of its internal energy throughout the process.

Due to the shape of the artery, the final stent diameter changes along its length. To find the average value, the diameter was measured at several cross sections. The SSS was expanded to 8.12 mm diameter and was predicted to have an average diameter of 7.0 ± 0.17 mm after recoil. Because of higher support of artery in the area between two segments, to reach the same final diameter as the SSS, the DSS was deployed to 7.43 mm diameter, resulting in an average diameter of 6.96 ± 0.08 mm after balloon deflation.

Table 1 Parameters used for material modeling of three layers of artery. The constants are based on 3rd order Moony-Rivlin hyper-elastic model. All units are in kPa [16].

	C10	C01	C20	C11	C30
Intima	18.8469	0.193 314	195.006	678.636	53.4141
Media	7.687 49	0	41.8209	11.5858	42.6237
Adventitia	0	5.499 99	0	0	151.227

Radial strength characterizes the ability of the stent to resist collapse under external load. The radial strengths of the stents were predicted as follows: An SSS and one of the segments of DSS were expanded to their nominal diameter. Then pressure was applied to the outer surface. The pressure at which a rapid inward deformation occurs was defined as radial strength. The radial strength was predicted for two types of stents.

Definitions. The *straightening index* was defined as the ratio of the artery's change in angle after stent implantation to the initial angle [7], see Fig. 1.

$$\text{The } \textit{percentage of straightening } = 100 * (\theta_{\text{initial}} - \theta_{\text{afterimplantation}}) / \theta_{\text{initial}}.$$

Results

The predicted Von Mises stress in the artery is concentrated at the outer curvature where the artery is in contact with the extremes of the SSS, see Fig. 2. This stress concentration is predicted in all three layers of the artery in this region. Among the three layers of artery, the intima is predicted to experience the highest level of stress with a maximum Von Mises stress of 325.9 kPa. The maximum level of stress in media and adventitia were 52.1 kPa and 20 kPa, respectively. The maximum stress within the stent after recoil is predicted to be 337.4 MPa (see Fig. 2(*a*)).

Stress concentrations are also predicted on the outer curvature of arterial wall at the extreme of the DSS after recoil, see Fig. 3. High magnitude of stress can also be seen at the inner curve of the artery between the crowns of the two segments of the DSS. Again the intima is predicted to bear the highest stress among the layers with maximum stress of 268.9 kPa. The maximum stress in the media and adventitia are about 46.54 kPa and 18.06 kPa, respectively. The maximum Von Mises stress in the stent strut is predicted to be 207.7 MPa.

To evaluate the differences between the levels of stress acting on the artery for the SSS and MSS, the volume of the artery under different levels of stress for two types of stents was also predicted, see Fig. 4. To the authors' knowledge, there is no experimental measurement of a threshold stress level to cause injury to different layers of the artery. Therefore, the volume of arterial tissue stressed at different levels were computed and compared. 20% of

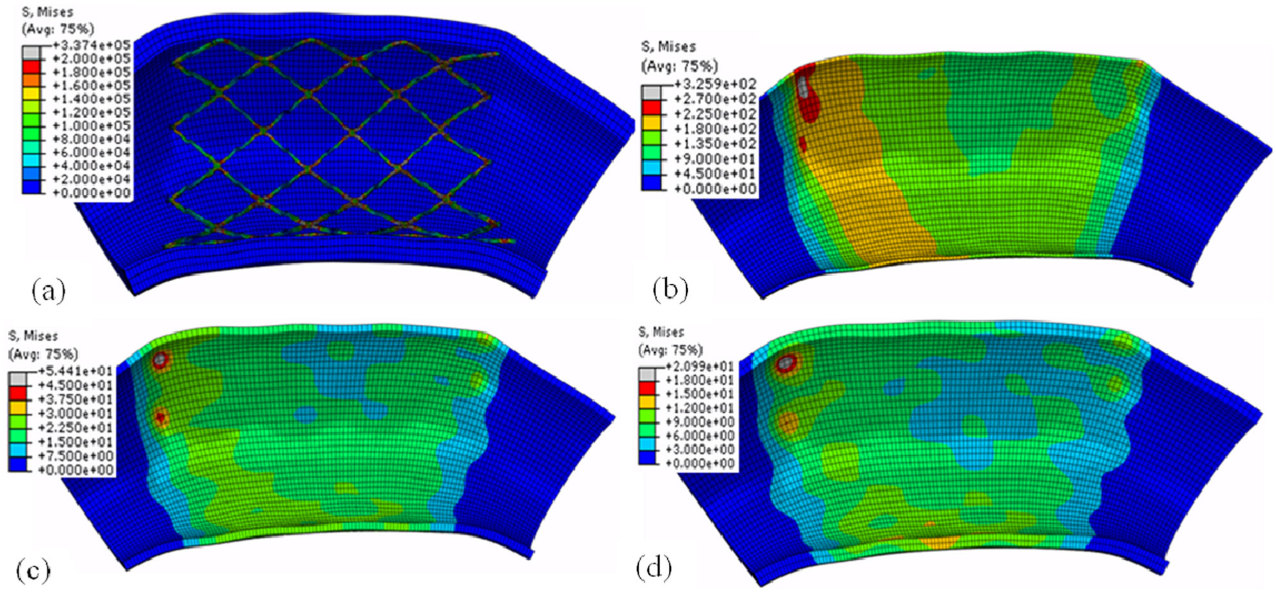

Fig. 2 Distribution of Von Mises stress in different layers of artery after recoil of expanded SSS. (*a*) Stent recoiled in the curved artery, (*b*) intima layer, (*c*) media, and (d) adventitia.

the volume of the intima was predicted to be stressed at high level stress (180–225 kPa) for SSS, compared to 4% for the DSS. Also, it was predicted that 25.7% of the volume of the media is stressed at a high stress level (22.5–30 kPa) compared to only 7.8% of the volume for the DSS. Similar trends of stress distribution are predicted in the adventia (see Figs. 2(*d*) and 3(*d*)).

Due to expansion of the stent in the artery, the artery tends to be straightened. Straightening is a result of a higher stent stiffness compared to the artery. The artery angle was measured as the angle between the two end faces of the artery (see Fig. 1). The angle of artery curvature is 90° before stent expansion. For the SSS this angle reduces to 69.5° after stenting, resulting in 22.8% straightening (based on definition defined in the literature [7]). In the case of DSS, the artery curve angle reduces to 76°, resulting in 15.5% straightening.

Stent conformity represents how well the stent sits on the artery wall. For both types of stents, separation between the stent and artery occurs at the extremes of the stents. The level of conformity; therefore, is defined as inverse of the largest distance between the outer surface of the stent and the inner surface of the artery. The levels of conformity were measured to be 6.37 mm^{-1} and 2.94 mm^{-1} for DSS and SSS, respectively.

The reduction in stent diameter due to the application of externally applied pressure was also predicted for the SSS and MSS (see Fig. 5. The changes in the diameter are gradual for both the SSS and MSS until the stent becomes unstable at higher pressures. This is predicted to occur at a slightly lower pressure for the MSS.

Discussion

The objective of this study was to use the finite element method to test the hypothesis that implanting nonoverlapping multiple stent segments into a curved artery would improve outcomes compared to implanting an SSS.

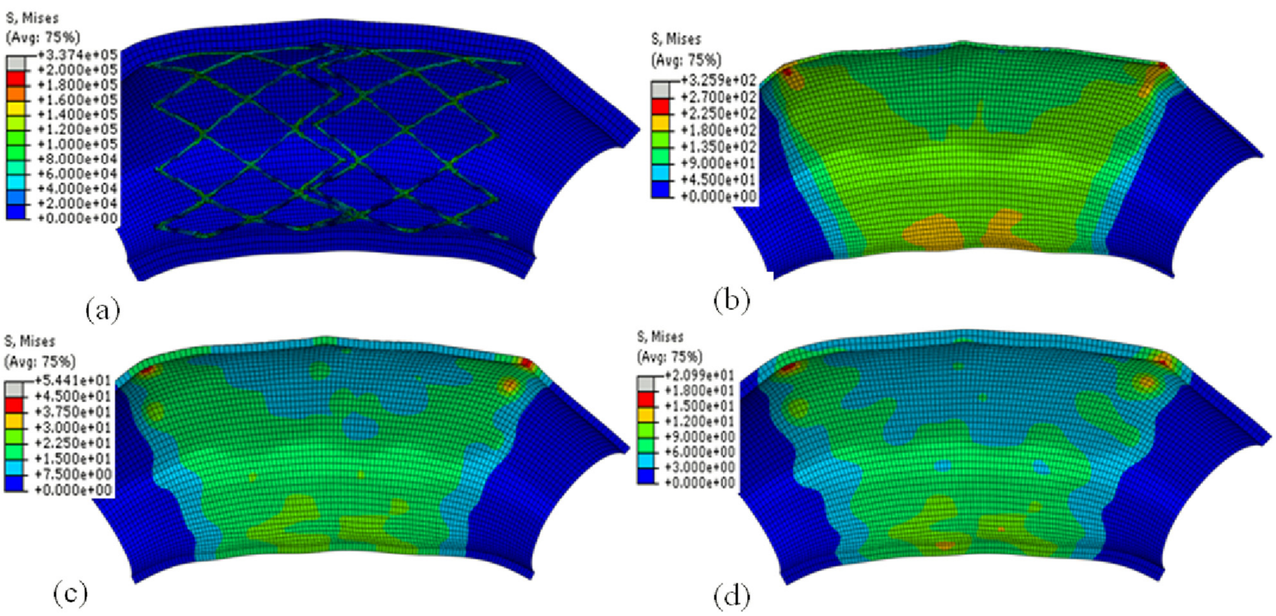

Fig. 3 Distribution of Von Mises stress in different layers of artery after recoil when a DSS is implanted. (*a*) Stent recoiled in the curved artery, (*b*) intima layer, (*c*) Media, (*d*) adventitia.

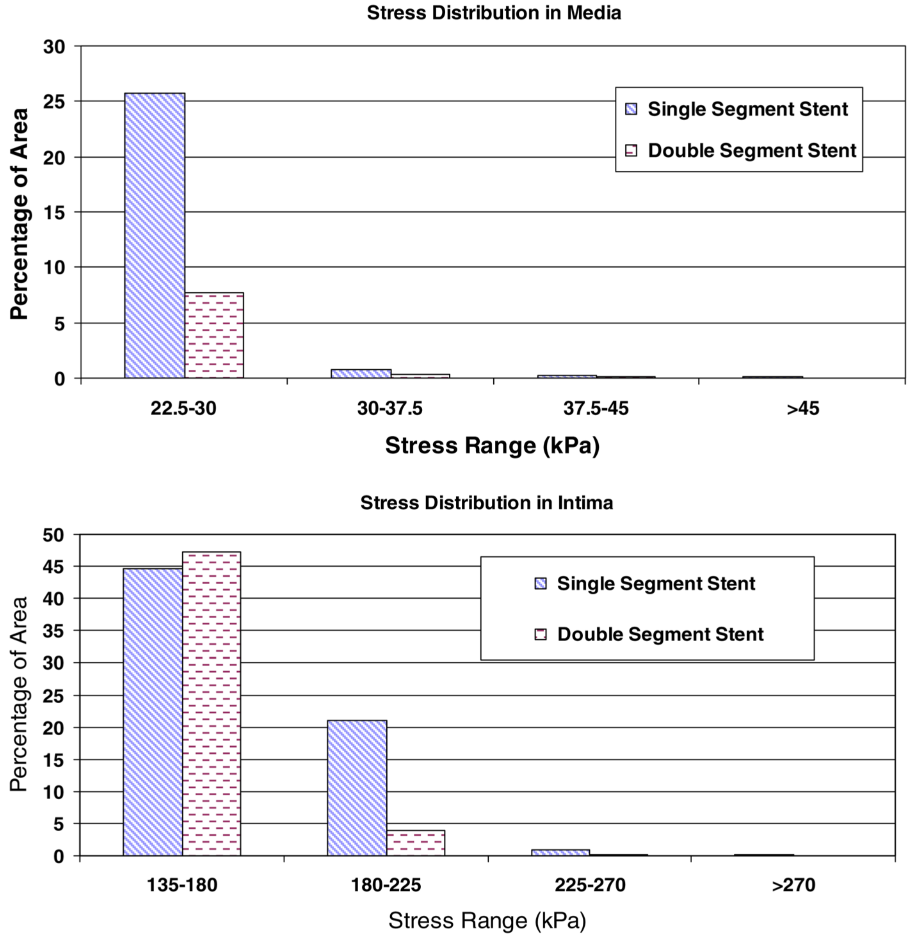

Fig. 4 Comparing the Von-Mises stress on intima and media for two different types of stents

This was determined by comparing predictions of key measures: Tissue stress levels (as a marker of injury), conformity, and radial strength. The results demonstrate the beneficial of implanting a DSS in comparison to an SSS, although significant work is still required to optimize such a new stent design, particularly in terms of the metal-to-artery ratio and the distance between the segments following deployment. Ensuring an adequate spacing between stent segments following deployment is critical to the success of a multiple segment approach as stent overlapping is known to contribute to stent wear and fatigue as well as ISR.

It is well documented that implanting a stent into a curved artery is more complicated compared to straight artery [8–10]. The high stiffness of a stent can cause straightening of a curved vessel. The results of this study show that there is a significant difference

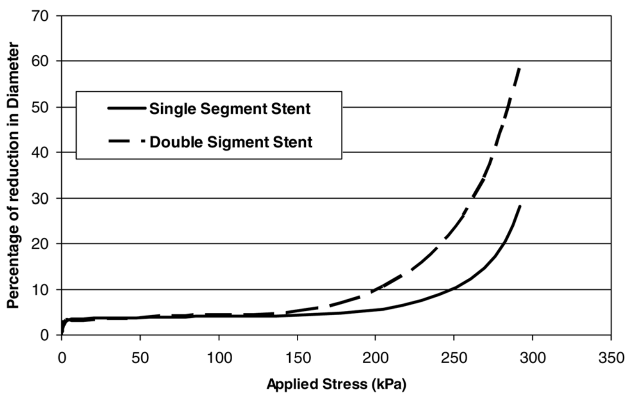

Fig. 5 Crush strength for the two types of stents

between the levels of straightening for the two types of stents. The level of straightening for an SSS is 28% greater than that for a DSS. This difference is expected to increase as the number of segments increases when compared to an SSS of total comparable length. As vessel straightening is known as a predictor for in-stent restenosis (ISR) and significantly contributes in occurrence of major advance cardiac event [18], the results of this study suggest that a multiple segment stent may reduce the risk of ISR compared with a similar SSS.

Due to different levels of recoil, the stents had to be expanded to different diameters in order to reach the same final diameter after unloading. The stent to artery diameter ratio for SSS and DSS were measured to be 1.35 and 1.23, respectively when inflated. In other words, the recoil of the stent is less when a two segment artery is used compared to an SSS. This may be due to the greater support provided to the artery by the interleaving of struts between the two segments of the DSS. The increased expansion of the SSS necessary to achieve the same final lumen gain will increase the stress on the artery and hence increase the risk of arterial injury [19].

After stent deployment, stress concentrations in the artery at the extremes of the stents were predicted for both the SSS and DSS. This effect has also been reported using a finite element simulation of a single segment stent in both curved and straight arteries [9]. However, the magnitude of the concentrated stress for a DSS is lower than that of the SSS. This difference is due to the higher flexibility of the DSS. As such stress concentrations are also correlated with ISR [20], the results further suggest a lower risk of ISR for the DSS. An increased volume of arterial tissue under lower levels of stress is also predicted for the DSS.

There is always a trade off between design requirements when developing a new stent. These requirements are often in conflict with each other. On the one hand, stents should be flexible enough to minimize vessel straightening after deployment and allow ease of placement, but on the other hand, they should provide sufficient radial strength to resist the compressive forces from the dilated vessel. Increasing flexibility while maintaining radial strength has proved extremely challenging with traditional stent designs. Comparing the two types of stents demonstrates that the radial strength of DSS is nearly comparable to an SSS. A significant advantage of a multiple segment stent is that the flexibility and radial strength can be controlled separately. Radial strength depends on the structural design of the segments and the flexibility depends on the segment length and the distance between them.

Fracture of stents is a continuing problem and is also correlated to the rate of ISR [21]. Its prevalence may also be increasing with the introduction of drug-eluting stents. Using a DSS instead of an SSS is also predicted to reduce the stress acting on the stent struts. Maximum Von Mises stress in the stent material reduced from 337.4 MPa for the SSS to 207.7 MPa for the DSS. Reduction in metal stress brings down the fracture risk for the stent struts. It is also expected that in stented arteries that are subjected to external mechanical forces such as compression and bending, higher stress will be generated within SSS compared to DSS as the latter can potentially better accommodate these externally applied loads.

Stent overlapping is a key concern when implanting multiple stents as it causes complications such as wearing of the stent segments, arterial injury, and higher rates of in-stent restenosis [22]. Recent studies show that the hazard ratio is significantly higher when multiple overlapping stents are implanted into a vessel compared with nonoverlapping stents. It has been also shown that the maximum restenosis occurs at the zone of overlapping [23,24]. Therefore, multiple segment stents should be designed such that no overlapping occurs while the artery is well supported.

The present study is limited in a number of ways. The constitutive model for the arterial tissue was based on experimental data [16]; however, the maximum stress predicted in the artery during expansion of the stent is beyond the experimental data. This means that the applied constitutive model may not reflect the real mechanical behavior of the tissue during implantation. Therefore, a constitutive model for higher range of stretch might be required when stent expansion is simulated. Additionally, the restenotic plaque has not been modeled. Also, arterial prestretch, residual stress, and luminal blood pressure were neglected. No consideration was given for tissue damage. While these limitations will affect the magnitude of the predicted stress distribution conditions, it is not expected to influence the overall findings of the study. Finally we have only considered a single artery (and stent) diameter and a unique degree and plane of curvature, as well as a single stent design. While the general findings of this study would be insensitive to small changes in diameter and curvature, clearly changes in stent design could impact upon the degree to which the DSS improves upon predicted outcome measures. Future studies adopting a design of experiment approach are required to address this question.

Conclusions

In conclusion, a DSS can provide increased flexibility without a significant reduction in radial strength compared to an SSS of similar total length. A DSS reduces the straightening of a curved artery as well as the stress levels within both the artery and stent struts. The stress is more evenly distributed on the artery wall when a DSS is used compared to an SSS. These advantages should theoretically reduce the risk of restenosis following stenting of a curved artery.

Acknowledgment

D.J.K. is a shareholder in Synergy Flow Ltd. D.J.K. and S.K. are co-inventors of patents licensed to Synergy Flow Ltd. This work is supported by Enterprise Ireland, CFTD2007-129.

References

[1] Tillich, M., Bell, R. E., Paik, D. S., Fleischmann, D., Sofilos, M. C., Logan, L. J., and Rubin, G. D., 2001, "Iliac Arterial Injuries After Endovascular Repair of Abdominal Aortic Aneurysms: Correlation with Iliac Curvature and Diameter," Radiology, **219**(1), pp. 129–136.

[2] Quinn, S. F., Kim, J., Sheley, R. C., and Frankhouse, J. H., 2001, "'Accordion' Deformity of a Tortuous External Iliac Artery After Stent-Graft Placement," Journal of Endovascular Therapy, **8**(1), pp. 93–98.

[3] Choi, G., Shin, L., K. Taylor, C. A., and Cheng, C. P., 2009, "In Vivo Deformation of the Human Abdominal Aorta and Common Iliac Arteries with Hip and Knee Flexion: Implications for the Design of Stent-Grafts," J. Endovascular Therapy, **16**(5), pp. 531–538.

[4] Schwartz, R. S., Huber, K. C., Murphy, J. G., Edwards, W. D., Camrud, A. R., Vlietstra, R. E., and Holmes, D. R., 1992, "Restenosis and the Proportional Neointimal Response to Coronary Artery Injury: Results in a Porcine Model," J. Am. Coll. Cardiol., **19**(2), pp. 267–274.

[5] Mitra, A. K., and Agrawal, D. K., 2006, "In Stent Restenosis: Bane of the Stent Era," J. Clin. Pathol., **59**(3), pp. 232–239.

[6] Kastrati, A., Mehilli, J., Dirschinger, J., Pache, J., Ulm, K., Schühlen, H., Seyfarth, M., Schmitt, C., Blasini, R., Neumann, F.-J., and Schömig, A., 2001, "Restenosis after Coronary Placement of Various Stent Types," Am. J. Cardiol., **87**(1), pp. 34–39.

[7] Abhyankar, A. D., Luyue, G., and Bailey, B. P., 1997, "Stent Implantation in Severely Angulated Lesions: Safety, Efficacy, and Morphological Remodelling," Cathet. Cardiovasc. Diagn., **40**(3), pp. 261–264.

[8] Ebrahimi, N., Claus, B., Lee, C. Y., Biondi, A., and Benndorf, G., 2007, "Stent Conformity in Curved Vascular Models with Simulated Aneurysm Necks Using Flat-Panel Ct: An in Vitro Study," AJNR Am. J. Neuroradiol., **28**(5), pp. 823–829.

[9] Wu, W., Wang, W.-Q., Yang, D.-Z., and Qi, M., 2007, "Stent Expansion in Curved Vessel and Their Interactions: A Finite Element Analysis," J. Biomech., **40**(11), pp. 2580–2585.

[10] Mortier, P., Holzapfel, G., De Beule, M., Van Loo, D., Taeymans, Y., Segers, P., Verdonck, P., and Verhegghe, B., 2009, "A Novel Simulation Strategy for Stent Insertion and Deployment in Curved Coronary Bifurcations: Comparison of Three Drug-Eluting Stents," Ann. Biomed. Eng., 38(1), pp. 88–99.

[11] Takashima, K., Kitou, T., Mori, K., and Ikeuchi, K., 2007, "Simulation and Experimental Observation of Contact Conditions Between Stents and Artery Models," Med. Eng. Phys., 29(3), pp. 326–335.

[12] Early, M., Lally, C., Prendergast, P. J., and Kelly, D. J., 2009, "Stresses in Peripheral Arteries Following Stent Placement: A Finite Element Analysis," Comput. Methods Biomech. Biomed. Eng., **12**(1), pp. 25–33.

[13] Liang, D. K., Yang, D. Z., Qi, M., and Wang, W. Q., 2005, "Finite Element Analysis of the Implantation of a Balloon-Expandable Stent in a Stenosed Artery," Int. J. Cardiol., 104(3), pp. 314–318.

[14] Wang, W.-Q., Liang, D.-K., Yang, D.-Z., and Qi, M., 2006, "Analysis of the Transient Expansion Behavior and Design Optimization of Coronary Stents by Finite Element Method," J. Biomech., **39**(1), pp. 21–32.

[15] Lally, C., Dolan, F., and Prendergast, P. J., 2005, "Cardiovascular Stent Design and Vessel Stresses: A Finite Element Analysis," J. Biomech., **38**(8), pp. 1574–1581.

[16] Schulze-Bauer, C. A. J., Morth, C., and Holzapfel, G. A., 2003, "Passive Biaxial Mechanical Response of Aged Human Iliac Arteries," J. Biomech. Eng., **125**(3), pp. 395–406.

[17] Wiersma, S., Dolan, F., and Taylor, D., 2006, "Fatigue and Fracture in Materials Used for Micro-Scale Biomedical Components," Biomed. Mater. Eng., **16**(2), pp. 137–146.

[18] Gyöngyösi, M., Yang, P., Khorsand, A., and Glogar, D., 2000, "Longitudinal Straightening Effect of Stents is an Additional Predictor for Major Adverse Cardiac Events," J. Am. Coll. Cardiol., **35**(6), pp. 1580–1589.

[19] Russo, R. J., Silva, P. D., and Yeager, M., 2007, "Coronary Artery Overexpansion Increases Neointimal Hyperplasia After Stent Placement in a Porcine Model," Heart, **93**(12), pp. 1609–15.

[20] Gu, L., Zhao, S., Muttyam, A. K., and Hammel, J. M., 2010, "The Relation Between the Arterial Stress and Restenosis Rate After Coronary Stenting," J. Med. Devices, **4**(3), p. 031005.

[21] Scheinert, D., Scheinert, S., Sax, J., Piorkowski, C., Braunlich, S., Ulrich, M., Biamino, G., and Schmidt, A., 2005, "Prevalence and Clinical Impact of Stent Fractures After Femoropopliteal Stenting," J. Am. Coll. Cardiol., **45**(2), pp. 312–315.

[22] Kastrati, A., Schomig, A., Elezi, S., Schuhlen, H., Dirschinger, J., Hadamitzky, M., Wehinger, A., Hausleiter, J., Walter, H., and Neumann, F. J., 1997, "Predictive Factors of Restenosis After Coronary Stent Placement," J. Am. Coll. Cardiol., **30**(6), pp. 1428–1436.

[23] Raber, L., Juni, P., Loffel, L., Wandel, S., Cook, S., Wenaweser, P., Togni, M., Vogel, R., Seiler, C., Eberli, F., Luscher, T., Meier, B., and Windecker, S., 2010, "Impact of Stent Overlap on Angiographic and Long-Term Clinical Outcome in Patients Undergoing Drug-Eluting Stent Implantation," J. Am. Coll. Cardiol., **55**(12), pp. 1178–88.

[24] Kereiakes, D. J., Wang, H., Popma, J. J., Kuntz, R. E., Donohoe, D. J., Schofer, J., Schampaert, E., Meier, B., Leon, M. B., and Moses, J. W., 2006, "Periprocedural and Late Consequences of Overlapping Cypher Sirolimus-Eluting Stents - Pooled Analysis of Five Clinical Trials," J. Am. Coll. Cardiol., **48**(1), pp. 21–31.